ARMY RESEARCH LABORATORY

Molecular Simulation of Shocked Materials Using Reaction Ensemble Monte Carlo: Part I. Application to Nitrogen Dissociation

by John K. Brennan and Betsy M. Rice

ARL-TR-3983 **November 2006**

Approved for public release; distribution is unlimited.

NOTICES

Disclaimers

The findings in this report are not to be construed as an official Department of the Army position unless so designated by other authorized documents.

Citation of manufacturer's or trade names does not constitute an official endorsement or approval of the use thereof.

Destroy this report when it is no longer needed. Do not return it to the originator.

Army Research Laboratory
Aberdeen Proving Ground, MD 21005-5066

ARL-TR-3983 **November 2006**

Molecular Simulation of Shocked Materials Using Reaction Ensemble Monte Carlo: Part I. Application to Nitrogen Dissociation

John K. Brennan and Betsy M. Rice
Weapons and Materials Research Directorate, ARL

Approved for public release; distribution is unlimited.

REPORT DOCUMENTATION PAGE

Form Approved
OMB No. 0704-0188

Public reporting burden for this collection of information is estimated to average 1 hour per response, including the time for reviewing instructions, searching existing data sources, gathering and maintaining the data needed, and completing and reviewing the collection information. Send comments regarding this burden estimate or any other aspect of this collection of information, including suggestions for reducing the burden, to Department of Defense, Washington Headquarters Services, Directorate for Information Operations and Reports (0704-0188), 1215 Jefferson Davis Highway, Suite 1204, Arlington, VA 22202-4302. Respondents should be aware that notwithstanding any other provision of law, no person shall be subject to any penalty for failing to comply with a collection of information if it does not display a currently valid OMB control number.
PLEASE DO NOT RETURN YOUR FORM TO THE ABOVE ADDRESS.

1. REPORT DATE *(DD-MM-YYYY)*	2. REPORT TYPE	3. DATES COVERED (From - To)
November 2006	Final	January 2005–May 2005

4. TITLE AND SUBTITLE
Molecular Simulation of Shocked Materials Using Reaction Ensemble Monte Carlo: Part I. Application to Nitrogen Dissociation

5a. CONTRACT NUMBER

5b. GRANT NUMBER

5c. PROGRAM ELEMENT NUMBER

6. AUTHOR(S)
John K. Brennan and Betsy M. Rice

5d. PROJECT NUMBER
H4311

5e. TASK NUMBER

5f. WORK UNIT NUMBER

7. PERFORMING ORGANIZATION NAME(S) AND ADDRESS(ES)
U.S. Army Research Laboratory
ATTN: AMSRD-ARL-WM-BD
Aberdeen Proving Ground, MD 21005-5066

8. PERFORMING ORGANIZATION REPORT NUMBER
ARL-TR-3983

9. SPONSORING/MONITORING AGENCY NAME(S) AND ADDRESS(ES)

10. SPONSOR/MONITOR'S ACRONYM(S)

11. SPONSOR/MONITOR'S REPORT NUMBER(S)

12. DISTRIBUTION/AVAILABILITY STATEMENT
Approved for public release; distribution is unlimited.

13. SUPPLEMENTARY NOTES

14. ABSTRACT
We demonstrate the applicability of the Reaction Ensemble Monte Carlo (RxMC) simulation method for calculating the shock Hugoniot properties of a material. The method does not require interaction potentials that simulate bond breaking or bond forming; it requires only the intermolecular potentials and the ideal-gas partition functions for the reactive species that are present. By performing Monte Carlo sampling of forward and reverse reaction steps, RxMC provides information on the chemical equilibria states of the shocked material including the density of the reactive mixture and the mole fractions of the reactive species. We illustrate the methodology for shocked liquid N_2, where we find excellent agreement with experimental measurements. This is the first of two reports describing the applicability of the RxMC method to simulating the shock Hugoniot properties of materials.

15. SUBJECT TERMS
molecular simulation, Monte Carlo, Hugoniot, reaction ensemble

16. SECURITY CLASSIFICATION OF:			17. LIMITATION OF ABSTRACT	18. NUMBER OF PAGES	19a. NAME OF RESPONSIBLE PERSON
a. REPORT	b. ABSTRACT	c. THIS PAGE			John K. Brennan
UNCLASSIFIED	UNCLASSIFIED	UNCLASSIFIED	UL	32	19b. TELEPHONE NUMBER (*Include area code*) 410-306-0678

Standard Form 298 (Rev. 8/98)
Prescribed by ANSI Std. Z39.18

Contents

List of Figures **iv**

List of Tables **iv**

Acknowledgments **v**

1. Introduction **1**

2. Methodology **3**

2.1 Reaction Ensemble Monte Carlo 3

2.2 Calculation of Shock Hugoniot Properties 5

3. Simulation Model and Details **7**

3.1 Intermolecular Potential Models 7

3.2 Simulation Details 8

4. Application **8**

5. Discussion **14**

6. References **15**

Distribution List **20**

List of Figures

Figure 1. Shock Hugoniot of liquid N_2. Calculated values from RxMC simulations using a reactive (○) and nonreactive (□) model are compared with experimental data (▲) (*54*, *55*). The shock pressure is plotted vs. the molar volume of N_2.....11

Figure 2. Shock Hugoniot of liquid N_2. Calculated values from RxMC simulations (reactive model: [○]; nonreactive model [□]) are compared with experimental data (▲) (*54*, *55*). The shock pressure is plotted vs. the shock wave velocity. 12

Figure 3. Species mole fractions (N_2: [♦]; N: [Δ]) along the Hugoniot curve determined from RxMC simulations of the N_2 dissociation reaction. 13

List of Tables

Table 1. Exponential-6 potential parameters. 7

Table 2. Initial fluid state used to evaluate equation 8. 9

Table 3. Constant-pressure RxMC simulations of shocked liquid N_2. 9

Table 4. Shock Hugoniot states of liquid nitrogen.[a] RxMC results are for the reactive model discussed in the text. Experimental data is taken from Nellis et al. (*55*), except for those noted. 11

Acknowledgments

The authors wish to thank Martin Lisal (Institute of Chemical Process Fundamentals, Academy of Sciences of the Czech Republic) for helpful discussions and critical reading of this manuscript. This work was performed while John K. Brennan held a National Research Council Research Associateship Award at the U.S. Army Research Laboratory. The calculations reported in this work were performed at the U.S. Army Research Laboratory Major Shared Resource Center, Aberdeen Proving Ground, MD.

INTENTIONALLY LEFT BLANK.

1. Introduction

The behavior of materials under conditions of extreme temperature and pressure is of critical importance in many fields of physics and fluid science (*1–3*). The properties of materials at these conditions can be measured through shock experiments, which are capable of producing pressures up to several hundred GPa and temperatures exceeding 10,000 K. Moreover, determining the shock properties of energetic materials is a crucial task in the field of detonation science (*4*).

Experimental measurements of the properties of shocked materials are often difficult because instrumentation must be capable of spanning a wide range of pressures (1–300 GPa) and temperatures (500–15000 K). Additionally, energy releases that might accompany a material under shock conditions, as well as the time and length scales over which the event occurs, have thwarted extensive experimental studies of many fundamental substances. As a further complication, recent theoretical predictions suggest that the detonation products of some systems supercritical phase separate, significantly altering the shock properties (e.g., references [*5–7*]. Unfortunately, current experimental techniques are not capable of delineating the phase separation of materials under shock conditions; thus, this behavior has yet to be verified.

Such laboratory challenges have necessitated the development of theoretical predictive capabilities to complement the experimental analyses. To date, the most reliable theoretical treatments for predicting shock properties apply statistical mechanical approaches such as variational perturbation theory (e.g., Ross [*8*] or integral equation theory (e.g., references [*9–11*]). These approaches predict the shock properties by minimizing the Gibbs free-energy and by requiring that the total number of elements constituting the chemically reacting species is conserved. Thermochemical software such as the chemical equilibrium code (*12*) and Cheetah (*13*) are capable of performing such calculations. However, these approaches require accurate equations of state (EOS) for the reactive mixture, thus limiting the prediction of the shock properties of materials to those for which equations of state are available. The calculations also require heats of formation and densities of the unshocked material. These quantities are often unknown for notional or novel energetic materials as well as for materials in highly nonideal environments (e.g., energetic materials packed in polymer matrices or confined in carbon nanotubes). Furthermore, approximations must often be made within the theoretical models to keep the calculations tractable, for example, to develop an analytical representation of the fluid equation of state (*11*) or in applying the van der Waals one-fluid approximation (*12*, *13*). These types of approximations can add uncertainty to the predictive capabilities of the methods.

A powerful simulation method available for studying the shock properties of materials while providing insight into atomic-level phenomena is the molecular dynamics (MD) method (*14–31*). The method can be used irrespective of rate limitations, the production of huge energy releases,

extreme thermodynamic conditions, or other regimes that are presently inaccessible by experimental methods. MD evaluation of the Hugoniot states of a material can be accomplished by calculating properties behind the shock discontinuity in a shockwave simulation (*30*) or by generating an EOS for subsequent evaluation of the Hugoniot conservation relations (*24*, *27*). Recently, an equilibrium MD method has been introduced, termed uniaxial Hugoniostat (*29*), which utilizes equations of motion that constrain the system during the MD simulation such that the time-averaged properties correspond to those on the shock Hugoniot curve. For evaluating the shock Hugoniot of a material, the uniaxial Hugoniostat technique is more efficient than the method of generating an EOS using standard MD for subsequent evaluation of the conservation equations (*24*, *27*). A significant drawback of all MD approaches, however, is that they require an accurate model of the interaction potential experienced between all species in the shocked and unshocked states. If the relative species concentrations of the products in the shocked state of interest are not known, then the MD approach requires an interaction potential that simulates bond breaking and bond formation in order to establish the chemical equilibrium of the final shocked state. Although significant advances have been made in developing potentials that reproduce the characteristics of a detonation, the potentials are still highly idealized representations of the energetic molecular system (*14–23*, *25–28*). However, if the relative species concentrations are known at the conditions of the shocked state, then generating the shock Hugoniot curve using either the conventional or the uniaxial Hugoniostat MD method only requires appropriate potentials that describe nonreacting interactions among all species present.

One of several alternative methods for calculating chemically reactive systems which is appropriate for determining the shock properties of materials is Reaction Ensemble Monte Carlo (RxMC) (*32*, *33*). RxMC circumvents some of the problems associated with conventional and uniaxial Hugoniostat MD methods. RxMC requires neither a priori knowledge of the relative concentrations of the species in the shocked state nor a potential that describes bond breaking or bond formation. The method only requires (a) functions that accurately describe nonreactive interactions between all possible species in the equilibrium mixture of the final shocked state (i.e., intermolecular potentials) and (b) ideal gas partition functions for all species in the mixture. For a given intermolecular potential model, the method will provide information on the chemical equilibrium state, such as the density of the reactive mixture, the mole fractions of reactive species, the change in the total number of moles, and the internal energy. The intermolecular model can contain various levels of detail including multisite molecules and electrostatic contributions. Numerous reactions can be simulated simultaneously in multiple phase systems by performing Monte Carlo sampling of forward and reverse reaction steps. Using the RxMC method, the dependence of the chemical equilibria on system conditions such as temperature, pressure, and the surrounding environment (e.g., a condensed phase or highly nonideal environment) can be studied.

In this work, we demonstrate the applicability of RxMC for calculating the shock Hugoniot properties of materials. We illustrate the method on shocked liquid N_2, which dissociates into atomic nitrogen (N) within a particular thermodynamic regime. This reaction has been studied extensively by both experimental and theoretical techniques. This report is the first of two reports that illustrate the RxMC method. In the second report (*34*), we consider shocked liquid NO, which is (nearly) an irreversible decomposition reaction that generates a mixture of homonuclear products (N_2 and O_2).

The outline of the report is as follows. The RxMC methodology applied to the simulation of the shock properties of materials is described in section 2. Simulation details and models can be found in section 3 and application of the method to shocked liquid N_2 is presented in section 4.

2. Methodology

2.1 Reaction Ensemble Monte Carlo

The RxMC method (32, 33) is designed to minimize the Gibbs free-energy, thus determining the true chemical equilibrium state irrespective of rate limitations. RxMC requires intermolecular potentials for the molecular species that are present in the reactive mixture and often uses spherically-averaged potentials such as Lennard-Jones or Exponential-6 models (35). RxMC also requires inputting the ideal-gas internal modes (vibration, rotation, and electronic) for each reactive species. These contributions can be included by calculating internal partition functions from molecular energy-level data (32) or by using tabulated thermochemical data (33). Regardless of the approach taken, the required information is readily available in standard sources (35–37) or can be generated using quantum mechanical calculations. Finally, the particular reactions occurring in the system must be specified. Provided that a sufficient set of independent reactions are specified, this requirement is not a considerably limiting factor since insignificant reactions are easily discernable by negligible product concentrations.

RxMC implementation provides information on the chemical equilibrium state, such as the density of the reactive mixture, mole fractions of reactive species, the change in the total number of moles, and the internal energy. RxMC can be performed in many different types of ensembles, including canonical, isothermal-isobaric, Gibbs (*38*), and other less common ensembles (*39*). Furthermore, RxMC can be performed for multiple reactions and multiple phases (*32*, *33*, *38*, *40–46*). RxMC does not simulate bond breaking or forming; these relatively rare events in standard Metropolis Monte Carlo (*47*) would result in considerable statistical uncertainty. Rather, RxMC directly samples forward and reverse reaction steps as Monte Carlo-type moves according to the stoichiometry of the reactions being sampled. The isothermal-

isobaric version of the RxMC method containing J number of reactions involves the following trial moves:

1. a change in the position or orientation of a molecule, chosen at random;
2. a forward step for randomly chosen reaction j, in which reactant molecules are chosen at random and changed to product molecules;
3. a reverse step for randomly chosen reaction j, in which product molecules are chosen at random and changed to reactant molecules; and
4. a random change in the simulation box volume.

Step 1 ensures that thermal equilibrium is established for the user-specified temperature, steps 2 and 3 ensure that chemical equilibrium is established, while step 4 satisfies the requirement of mechanical equilibrium for the user-specified pressure. Note that the transition probabilities in steps 2 and 3 do not require specifying the values of the chemical potentials nor chemical potential differences for any of the mixture components.

The acceptance probability of state k going to state l for a particle displacement or orientation step is given by

$$P_{kl}^{dis} = \min\{1, \exp(-\beta \Delta U_{kl})\}, \tag{1}$$

where $\Delta U_{kl} = U_l - U_k$ is the change in the configurational energy and $\beta = 1/k_B T$; k_B is the Boltzmann constant and T is the temperature.

The acceptance probability for a reaction step is given by

$$P_{j,kl}^{rxn} = \min\left\{1, \prod_{i=1}^{c_j} \frac{N_i!}{(N_i + \nu_{ji}\xi_j)!} \left(\frac{q_{\text{int},i} V}{\Lambda_i^3}\right)^{\nu_{ji}\xi_j} \exp(-\beta \Delta U_{kl})\right\}, \tag{2}$$

where c_j is the total number of species in reaction j; N_i is the total number of molecules of species i; ν_{ji} is the stoichiometric coefficient of species i in reaction j; ξ_j is the molecular extent of reaction for reaction j; $q_{\text{int},i}$ is the quantum partition function for the internal modes of an isolated molecule of species i, which includes vibrational, rotational, and electronic; Λ_i is the thermal de Broglie wavelength of species i; and V is the total volume of the system. Equation 2 is appropriate for both forward and reverse reaction steps ($\xi_j = 1$ for a forward step and $\xi_j = -1$ for a reverse step), where the stoichiometric coefficients are taken to be positive for product species and negative for reactant species. (For example, consider the reaction A⇔2B. For the reaction as written, the stoichiometric coefficients for species A and B are $\nu_A = -1$ and $\nu_B = +2$ while $\xi = +1$. Then for the reverse reaction step, ν_A and ν_B again are –1 and +2, respectively, but now $\xi = -1$.)

Finally, a random change in the simulation box volume is accepted with the probability

$$P_{kl}^{vol} = \min\left\{1, \exp\left(-\beta\Delta U_{kl} - \beta P_{imp}(V_l - V_k) + N \ln\frac{V_l}{V_k}\right)\right\}, \tag{3}$$

where P_{imp} is the user-specified, or imposed, pressure. Derivations of these transition probabilities along with further details of the methodology can be found in the original papers (*32*, *33*, *38*).

2.2 Calculation of Shock Hugoniot Properties

The thermodynamic quantities of a material in the initial unshocked state and the final shocked state are related by the conservation equations of mass, momentum, and energy across the shock front as follows (*4*):

$$\text{Mass:} \quad \rho_o D = \rho(D - u). \tag{4}$$

$$\text{Momentum:} \quad P - P_o = \rho_o u D. \tag{5}$$

$$\text{Energy:} \quad E - E_o = \tfrac{1}{2}(P + P_o)(V_o - V)\ . \tag{6}$$

In equations 4–6, E is the specific internal energy, P is the pressure, ρ is the specific density, $V = 1/\rho$ is the specific volume, D is the velocity of the shock wave propagating through the material, and u is the mass velocity of the products behind the shock wave. The term "specific" refers to the quantity per unit mass, while the subscript "o" refers to the quantity in the initial unshocked state.

The shock wave velocity D can be calculated by solving equations 4 and 5 for the mass velocity u and equating these expressions. The resulting expression, termed the Rayleigh line, can be written as

$$R = \rho_o^2 D^2 - (P - P_o)(V_o - V) = 0\ . \tag{7}$$

The so-called *Hugoniot* function satisfies equation 6 as

$$\mathrm{H_g}(T,V) = 0 = E - E_o - \tfrac{1}{2}(P + P_o)(V_o - V)\ . \tag{8}$$

Note that the quantities E and V are extensive quantities in equations 6–8 and thus dependent on the relative amounts of the reactive species. The extensive quantities used in this work were formulated on a specific basis (per gram); alternatively, these quantities can be formulated on a total system basis (total number of moles). The relative amounts of the reactive species along with the quantities E, P, and V are calculated explicitly during the RxMC simulation. The internal energy is calculated during the RxMC simulation based upon the following derivation. The thermodynamic definition of the internal energy is given as

$$E \equiv H - PV\ , \tag{9}$$

where H is the specific enthalpy that can be written as a sum of the ideal-gas (H^{o}) and excess enthalpies (H^{e}):

$$H = H^{\mathrm{o}} + H^{\mathrm{e}} . \tag{10}$$

The ideal-gas and excess enthalpies can be written as

$$H^{\mathrm{o}} = \sum_{i=1}^{c_j} \mathrm{y}_i H_i^{\mathrm{o}} \tag{11}$$

and

$$H^{\mathrm{e}} = U^{\mathrm{conf}} + PV - \mathrm{R}T , \tag{12}$$

so that

$$H = \sum_{i=1}^{c_j} \mathrm{y}_i H_i^{\mathrm{o}} + U^{\mathrm{conf}} + PV - \mathrm{R}T . \tag{13}$$

U^{conf} is the total configurational energy calculated during the simulation from the species-species interactions; y_i is the mole fraction of species i; c_j is the total number of species; H_i^{o} is the specific ideal-gas enthalpy of pure species i, which can be determined solely from tabulated thermochemical data at the appropriate temperature, T (*37*, *48*, *49*), or with tabulated thermochemical data supplemented with computed values where data is lacking (e.g., [*50*, *51*]); and R is the universal gas constant. Substituting equation 13 into equation 9,

$$E = \sum_{i=1}^{c_j} \mathrm{y}_i H_i^{\mathrm{o}} + U^{\mathrm{conf}} - \mathrm{R}T , \tag{14}$$

which is the specific internal energy expression needed in equation 8.

The search algorithm for locating a point on the Hugoniot curve used in this study is as follows:

Step 1: For a user-specified pressure, P, a few RxMC-NPT simulations were performed at temperatures believed to be near Hg(T,V) = 0.

Step 2: A functional form for the Hg vs. T plot is determined, e.g., fitted to a quadratic polynomial, and the temperature (T_{Hg}) that satisfies equation 8 at Hg = 0 is interpolated.

Step 3: Similarly, functional forms for the other desired quantities (V, E, D) were determined and interpolated at T_{Hg}.

Depending on the initial guess of T_{Hg}, additional RxMC simulations may be required to achieve the desired accuracy. Typically, 4–6 RxMC simulations are needed to determine a single point on the Hugoniot curve, where best results are obtained when chosen values of T include both $\mathrm{H_g}>0$ and $\mathrm{H_g}<0$. Steps 1–3 are then repeated to trace out the entire Hugoniot curve.

3. Simulation Model and Details

3.1 Intermolecular Potential Models

The species particles interact through the exponential-six potential, which can be expressed as:

$$U_{\exp-6}(r) = \begin{cases} \infty & r < r_{\text{core}} \\ \dfrac{\varepsilon}{1 - 6/\alpha}\left[\dfrac{6}{\alpha}\exp\left(\alpha\left[1 - \dfrac{r}{r_m}\right]\right) - \left(\dfrac{r_m}{r}\right)^6\right] & r \geq r_{\text{core}} \end{cases} , \tag{15}$$

where ε is the depth of the attractive well between particles, r_m is the radial distance at which the potential is a minimum, while α controls the steepness of the repulsive interaction. The cutoff distance r_{core} is included to avoid the unphysical singularity in the potential function as r→0. The potential parameters for the species considered in this work are given in table 1. A spherical cutoff of $2.5r_{m,\text{N2}}$ was applied with long range corrections added to account for interactions beyond this distance (*52*). Electrostatic contributions were ignored between species. The unlike interactions between species *i* and *j* were approximated by the Lorentz-Berthelot mixing rules (*35*) for ε_{ij}, α_{ij}, and $r_{m,ij}$:

$$\varepsilon_{ij} = (\varepsilon_i\varepsilon_j)^{1/2} ;\ \alpha_{ij} = (\alpha_i\alpha_j)^{1/2} ;\ r_{m,ij} = (r_{m,i} + r_{m,j})/2 ,$$

while

$$r_{\text{core},ij} = (r_{\text{core},i} + r_{\text{core},j})/2 . \tag{16}$$

Table 1. Exponential-6 potential parameters.

Species	r_{core} (Å)	r_m (Å)	ε/k_B (K)	α	Source (Reference No.)
N_2	1.13	4.2005	101.10	12.684	(*11*)
N	0.98	2.5688	88.181	11.013	(*11*)

The vibrational and rotational contributions to the ideal-gas partition function of N_2 used in simulating the N_2 dissociation reaction were calculated using a standard source (*36*) and supplemented with electronic level constants that included the ground state and six excited electronic states (*48*). For N, the electronic energy levels were taken from Moore and Gallagher (*49*). The corresponding thermochemical reference data were used in calculating the ideal-gas enthalpies (H_i^o) required in equation 11 (*37*, *48*, *49*).

3.2 Simulation Details

Constant-pressure RxMC simulations of shocked N_2 were initiated from 3375 N_2 particles placed on a face-centered-cubic lattice structure. The standard periodic boundary conditions and minimum image convention were used (*53*). Simulations were performed in steps, where a step (chosen with equal probability) was either a particle displacement, forward reaction step, or reverse reaction step. A change in the simulation cell volume was attempted every 2500 steps. Simulations were equilibrated for 0.3×10^7 steps after which averages of the quantities were taken over 2.0×10^7 steps. Uncertainties were estimated using the method of block averages by dividing the production run into 10 equal blocks (*52*). Reported uncertainties are one standard deviation of the block averages. The maximum displacement and volume change were adjusted to achieve an acceptance fraction of ~0.33 and 0.5, respectively. Depending on the system conditions, the acceptance fraction of the reaction steps ranged from 0.075–0.375. Calculated quantities were reduced by the exponential-6 potential energy (ε) and size (r_m) parameters of N_2.

4. Application

We consider shocked N_2 in the pressure range 3–90 GPa for which reliable experimental data are available (*54*, *55*). At pressures between ~30–100 GPa, the N≡N triple bond is destabilized and molecular nitrogen dissociates into atomic nitrogen (*56*, *57*). At higher pressures, theory suggests that nitrogen can exist as a metastable polymeric phase of N atom clusters that are covalently bonded (*58–62*), before losing this covalency at still higher pressures. In the present work, we consider only the regime where molecular nitrogen is believed to dissociate into atomic nitrogen, $N_2 \Leftrightarrow 2N$. Analogous to the work of Fried and Howard (*11*), we consider two models for this reaction, a reactive model that includes the dissociation reaction, and a nonreactive model that does not.

We determined the shock Hugoniot properties of liquid N_2 using the calculated initial states given in table 2. The values given in table 2 were determined by performing a canonical ensemble (constant-N*VT*) Monte Carlo simulation of N = 3375 N_2 molecules at $T = 77.0$ K and at a specific volume of $V = 1.238$ cm^3/g. A comparison of the pressure and internal energy determined from this N*VT* simulation with experiment is given in table 2. The shock Hugoniot properties were determined by carrying out the prescription outlined in section 2.2. The raw data determined from a series of constant-pressure RxMC simulations at several different temperatures are given in table 3. Also reported in table 3 are the values of the Hugoniot expression (equation 8) using the predicted thermodynamic data. Quadratic polynomials were used in the fitting procedure of steps 2 and 3 (see section 2.2) with the exception of the shock wave velocity (D), where a linear equation was used. A comparison of the shock properties along the principal Hugoniot calculated from the RxMC simulations and the available

Table 2. Initial fluid state used to evaluate equation 8.

Thermodynamic Property	**Liquid N_2**	
	Experiment (*55*)	**N*VT*-MC**
Temperature, T (K)	77.0 ± 0.5	77.0
Density, ρ (g/cm^3)	0.808 ± 0.003	0.808
Pressure, P (MPa)	—	50.49 ± 0.02
Energy, E (kJ/g)	—	–0.441 ± 0.004

Table 3. Constant-pressure RxMC simulations of shocked liquid N_2.

T (K)	**<*P*> (GPa)**	**Mole Fraction[a]**		**<*V*> (cm^3/g)**	**<U^{conf}> (kJ/g)**	**H^{ob} (kJ/g)**	**E^c (kJ/g)**	**H_g^d (kJ/g)**	**D^e (km/s)**
		<x(N_2)>	**< x(N)>**						
P_{imp} = 2.96 GPa									
475	3.010(2)	1.0000	0.0000	0.7532(8)	0.182(2)	0.1852	0.227	–0.0732	3.059
500	3.008(1)	1.0000	0.0000	0.7572(7)	0.188(2)	0.2110	0.250	–0.0429	3.071
525	3.008(2)	1.0000	0.0000	0.7606(9)	0.192(3)	0.2379	0.274	–0.0138	3.082
550	3.008(2)	1.0000	0.0000	0.7646(9)	0.197(3)	0.2643	0.298	0.0165	3.094
P_{imp} = 4.74 GPa									
850	4.795(3)	1.0000	0.0000	0.7047(6)	0.463(4)	0.5955	0.806	–0.0433	3.693
900	4.795(3)	0.9998(1)	0.0002(1)	0.7090(8)	0.471(3)	0.6566	0.860	0.0210	3.708
950	4.790(3)	0.9997(1)	0.0003(1)	0.7132(6)	0.478(5)	0.7201	0.916	0.0879	3.721
P_{imp} = 10.0 GPa									
1950	10.072(7)	1.0000	0.0000	0.6197(9)	1.249(7)	1.9407	2.611	–0.0751	4.984
2000	10.081(4)	0.9998(1)	0.0002(1)	0.6210(6)	1.254(9)	2.0101	2.670	–0.0115	4.992
2050	10.066(8)	0.9998(1)	0.0002(1)	0.6235(6)	1.260(9)	2.0749	2.726	0.0609	4.998
P_{imp} = 18.1 GPa									
3850	18.195(2)	0.9997(1)	0.0003(1)	0.5549(7)	2.398(2)	4.4512	5.707	–0.0806	6.380
3900	18.191(2)	0.9997(1)	0.0003(1)	0.5557(7)	2.401(1)	4.5179	5.761	–0.0168	6.383
3950	18.189(2)	0.9997(1)	0.0003(1)	0.5569(8)	2.407(2)	4.5851	5.820	0.0533	6.388
P_{imp} = 29.9 GPa									
6700	30.023(2)	0.9930(1)	0.0070(1)	0.5001(8)	3.963(1)	8.5267	10.502	–0.1103	7.890
6725	30.015(2)	0.9939(1)	0.0061(1)	0.5017(8)	3.960(2)	8.5392	10.503	–0.0810	7.897
6750	30.008(3)	0.9936(1)	0.0064(1)	0.5024(7)	3.966(3)	8.5808	10.543	–0.0274	7.900
6775	30.009(2)	0.9926(1)	0.0075(1)	0.5008(7)	3.954(2)	8.6431	10.586	–0.0089	7.892
6800	30.022(2)	0.9923(1)	0.0077(1)	0.5010(7)	3.957(1)	8.6847	10.624	0.0271	7.895
P_{imp} = 36.0 GPa									
7900	36.083(3)	0.9762(1)	0.0238(1)	0.4762(9)	4.666(2)	10.8830	13.204	–0.1105	8.514
7950	36.121(3)	0.9753(1)	0.0247(1)	0.4765(6)	4.672(2)	10.9868	13.299	–0.0252	8.520
7975	36.100(2)	0.9750(1)	0.0250(1)	0.4766(5)	4.668(2)	11.0363	13.338	0.0233	8.518
8000	36.143(2)	0.9744(1)	0.0256(1)	0.4766(5)	4.677(2)	11.0924	13.395	0.0644	8.523
8050	36.141(2)	0.9734(1)	0.0266(1)	0.4768(7)	4.675(2)	11.2008	13.486	0.1606	8.524
8475	36.120(3)	0.9648(1)	0.0352(1)	0.4796(11)	4.686(2)	12.1361	14.307	1.0393	8.537
8500	36.115(3)	0.9643(1)	0.0357(1)	0.4796(5)	4.682(2)	12.1932	14.352	1.0863	8.536
8550	36.119(3)	0.9632(1)	0.0368(1)	0.4800(8)	4.687(2)	12.3059	14.455	1.1950	8.539

Table 3. Constant-pressure RxMC simulations of shocked liquid N_2 (continued).

T (K)	<*P*> (GPa)	Mole Fraction[a] <x(N_2)>	< x(N)>	<*V*> (cm^3/g)	<U^{conf}> (kJ/g)	H^{ob} (kJ/g)	E^c (kJ/g)	H_g^d (kJ/g)	D^e (km/s)
P_{imp} = 47.0 GPa									
9350	47.152(5)	0.9260(1)	0.0741(1)	0.4351(8)	5.809(3)	14.9046	17.939	–0.5608	9.481
9450	47.182(2)	0.9221(2)	0.0779(2)	0.4352(6)	5.812(2)	15.2050	18.212	–0.2958	9.485
9550	47.148(2)	0.9183(2)	0.0816(2)	0.4355(3)	5.805(2)	15.5024	18.473	–0.0142	9.484
9575	47.130(2)	0.9179(1)	0.0821(1)	0.4355(3)	5.799(2)	15.5580	18.515	0.0353	9.482
9600	47.134(3)	0.9166(2)	0.0834(2)	0.4357(6)	5.804(2)	15.6475	18.602	0.1249	9.483
P_{imp} = 52.6 GPa									
9500	52.740(4)	0.9101(2)	0.0899(2)	0.4160(6)	6.336(3)	15.7319	19.248	–1.9974	9.911
9750	52.737(3)	0.9002(2)	0.0998(2)	0.4162(4)	6.325(2)	16.5027	19.934	–1.3053	9.912
10000	52.754(3)	0.8888(2)	0.1112(2)	0.4162(4)	6.314(3)	17.3362	20.683	–0.5620	9.914
10250	52.755(6)	0.8774(2)	0.1226(2)	0.4164(8)	6.304(4)	18.1791	21.441	0.2006	9.915
P_{imp} = 60.4 GPa									
10400	60.527(3)	0.8498(3)	0.1502(3)	0.3925(5)	6.989(2)	19.4771	23.379	–1.7771	10.469
10500	60.521(4)	0.8441(2)	0.1559(2)	0.3924(5)	6.979(2)	19.8615	23.724	–1.4344	10.468
10600	60.563(7)	0.8388(3)	0.1612(3)	0.3920(8)	6.969(4)	20.2337	24.057	–1.1294	10.469
10900	60.551(4)	0.8231(2)	0.1769(2)	0.3916(7)	6.939(2)	21.3514	25.056	–0.1370	10.466
10950	60.506(3)	0.8201(3)	0.1799(3)	0.3916(6)	6.928(4)	21.5531	25.231	0.0583	10.462
11000	60.544(4)	0.8170(4)	0.1830(4)	0.3915(8)	6.929(2)	21.7593	25.424	0.2306	10.465
P_{imp} = 81.1 GPa									
12400	81.093(5)	0.6487(4)	0.3513(4)	0.3352(5)	8.275(4)	30.8436	35.438	–0.7344	11.728
12500	81.075(7)	0.6416(5)	0.3584(5)	0.3347(7)	8.253(3)	31.3115	35.854	–0.3281	11.724
12600	81.120(8)	0.6351(4)	0.3649(4)	0.3343(8)	8.240(4)	31.7590	36.259	0.0387	11.724
P_{imp} = 91.5 GPa									
13000	91.191(9)	0.5584(6)	0.4416(6)	0.3109(7)	8.775(5)	35.5438	40.461	–1.3754	12.274
13250	91.118(9)	0.5424(5)	0.4576(5)	0.3101(8)	8.725(4)	36.6715	41.464	–0.3756	12.263
13500	91.092(11)	0.5267(7)	0.4733(7)	0.3092(8)	8.671(6)	37.7904	42.454	0.5857	12.255
15500	90.482(12)	0.4170(6)	0.5830(6)	0.3045(11)	8.242(3)	46.2912	49.933	8.1337	12.183
16000	90.418(14)	0.3917(6)	0.6083(6)	0.3036(12)	8.147(4)	48.3805	51.779	9.9691	12.173
16500	90.064(18)	0.3599(8)	0.6401(8)	0.3022(17)	7.991(4)	50.7644	53.858	12.1530	12.141

Notes: '< >' indicates ensemble averages determined from the simulation.
Uncertainty in units of the last decimal digit is given in parentheses: 3.010(2) means 3.010 ± 0.002.
[a]Mole fraction of N_2, so $x(N_2) = N_{N2}/N_{total}$ and $x(N) = ½ N_N/N_{total}$, where N total = 3375.
[b]From equation 11.
[c]From equation 14.
[d]From equation 8.
[e]From equation 7.

experimental data is given in table 4. In table 4, the uncertainties for the shock Hugoniot properties measured by experiment are given in parentheses, while the uncertainties in the RxMC calculations can be estimated from the R-square value of the functional fit of data given in table 3. Typical R-square values for the predicted temperatures and specific volumes are 0.97–0.99. Plots of the shock Hugoniot pressure vs. the specific volume and the shock wave velocity are given in figures 1 and 2, respectively, for both the reactive and nonreactive models.

Table 4. Shock Hugoniot states of liquid nitrogen.[a] RxMC results are for the reactive model discussed in the text. Experimental data is taken from Nellis et al. (*55*), except for those noted.

P **(GPa)**		***V*** **(cm^3/mol N_2)**		***T*** **(K)**		***D*** **(km/s)**	
Exp.	**RxMC[b]**	**Exp.**	**RxMC**	**Exp.**	**RxMC**	**Exp.**	**RxMC**
2.96[c]	2.96	21.7	21.36	—	536.2	3.14	3.087
4.74[c]	4.74	20.1	19.82	—	883.9	3.74	3.703
10.1[c]	10.0	17.3	17.41	—	2008.4	5.00	4.993
18.1(0.5)	18.1	15.34(0.5)	15.57	4300(200)	3912.4	6.34	6.384
29.9(0.5)	29.9	14.26(0.5)	14.05	7300(250)	6778.1	7.93	7.895
36.0(0.4)	36.0	13.41(0.4)	13.35	8750(300)	7963.0	8.52	8.519
47.0(0.5)	47.0	11.83(0.5)	12.20	8900(600)	9557.7	9.40	9.483
52.6(0.5)	52.6	11.13(0.5)	11.66	11100(800)	10185.4	9.79	9.914
60.4(0.7)	60.4	10.31(0.7)	10.97	12000(850)	10935.2	10.31	10.465
81.1(1.5)	81.1	9.40(1.5)	9.366	14500(1000)	12588.9	11.73	11.724

[a]Uncertainties in experimental data (where available) are given in parentheses.
[b]Pressure imposed in the constant-pressure version of the RxMC method.
[c]Taken from Zubarev and Telegin (*54*).

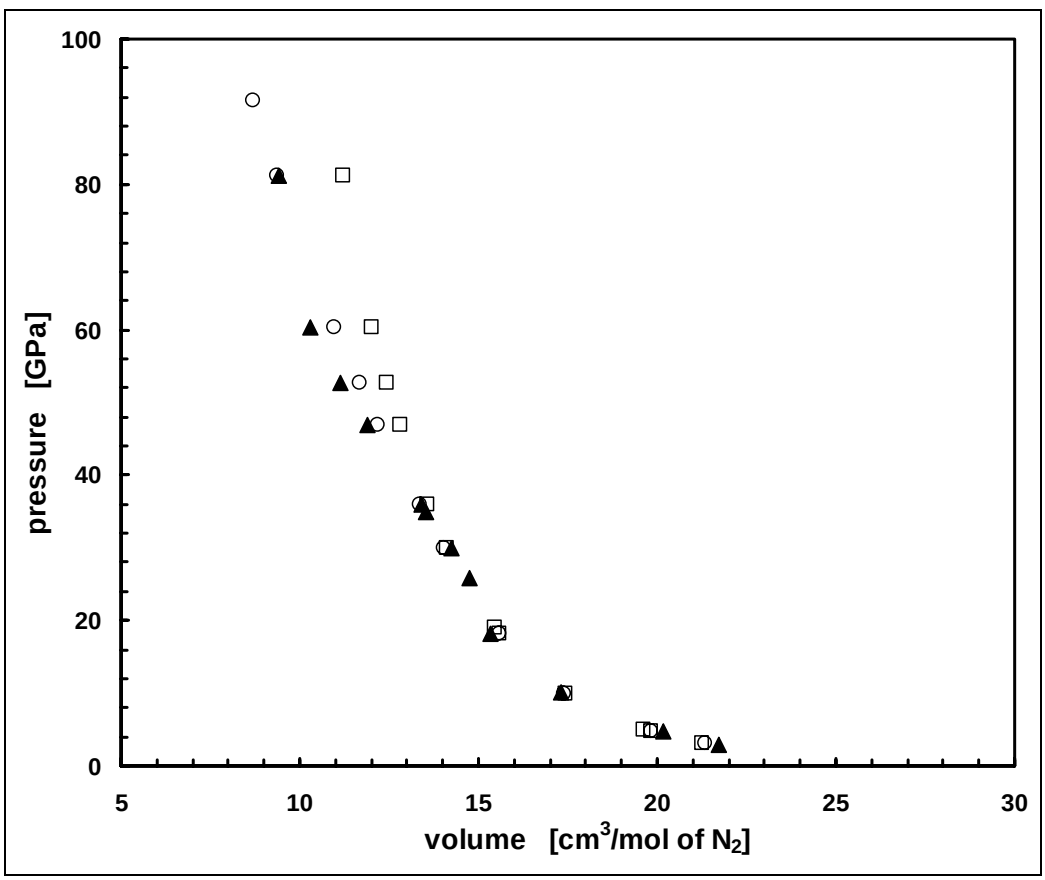

Figure 1. Shock Hugoniot of liquid N_2. Calculated values from RxMC simulations using a reactive (○) and nonreactive (□) model are compared with experimental data (▲) (*54*, *55*). The shock pressure is plotted vs. the molar volume of N_2.

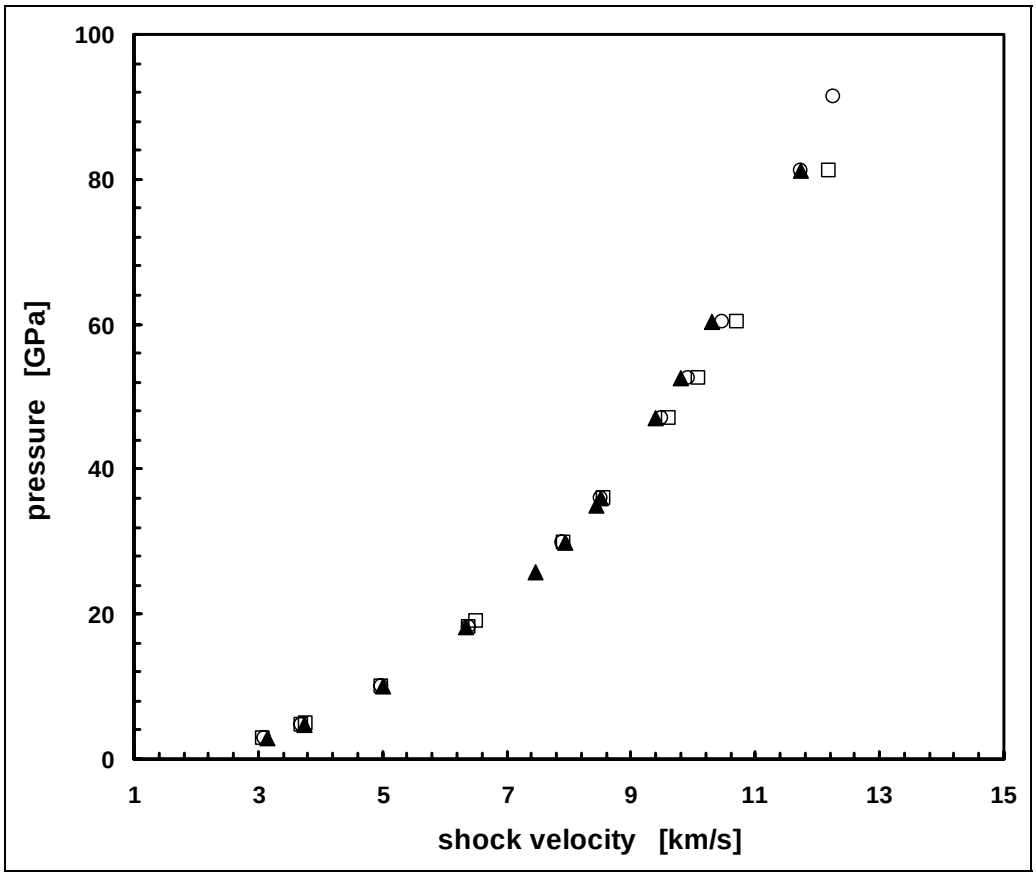

Figure 2. Shock Hugoniot of liquid N_2. Calculated values from RxMC simulations (reactive model: [○]; nonreactive model [□]) are compared with experimental data (▲) (*54*, *55*). The shock pressure is plotted vs. the shock wave velocity.

We found excellent agreement between the RxMC calculations using the reactive model and the experimental measurements for most of the pressures considered. As the pressure is increased along the Hugoniot, the system becomes a partially dissociated fluid containing a mixture of N_2 molecules and N atoms. This behavior is reflected in the species mole fractions plot of figure 3. Values of the mole fractions shown in figure 3 were determined by interpolating the data reported in table 3 to T_{Hg} using a quadratic function. It is evident from figure 1 that the nonreactive model fails at high pressures where the dissociation is not negligible (*11*).

The experimental data appears to exhibit a softening of the Hugoniot curve near 55 GPa while the RxMC simulations do not predict this behavior. Experimental errors are increasing in this region; therefore, whether the discrepancy is due to experimental uncertainty or an inaccurate model cannot be conclusively established (*11*). Interestingly, however, recent density-functional theory (DFT) calculations (*31*) predict the softening behavior. Pair correlation calculations in the work of Kress et al. (*31*) indicate that the system contains a small fraction of clusters larger than dimers in the partially dissociated region; however, these larger clusters are not long-lived. The dissociated system may contain N_n molecules bound by single (N–N) or single and double

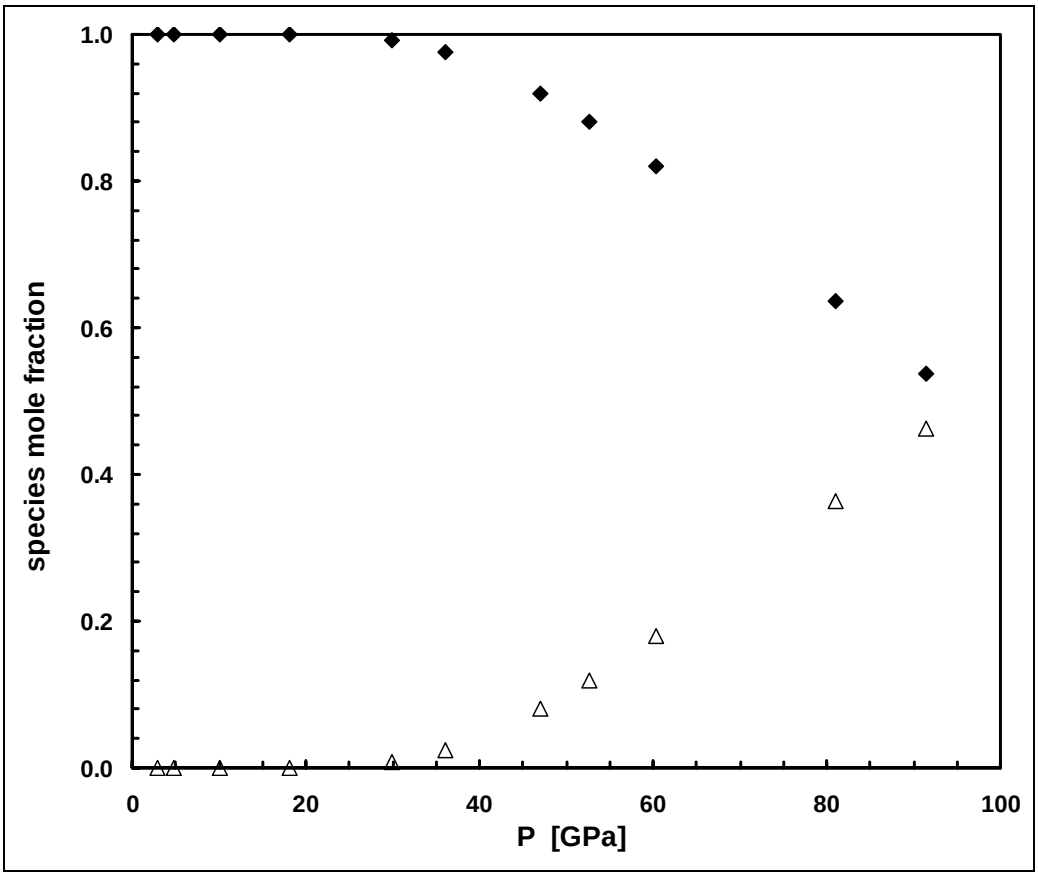

Figure 3. Species mole fractions (N_2: [♦]; N: [Δ]) along the Hugoniot curve determined from RxMC simulations of the N_2 dissociation reaction.

N ═ N) bonds. Although refining the N_2 model is outside the scope of the present work, such products and their accompanying reactions could be included into the RxMC simulation scenario, e.g., N ≡ N⇔N ═ N or N ≡ N⇔N–N, which may make RxMC calculations more compatible with the experimental measurements.

As a matter of curiosity, a point along the Hugoniot curve at P = 91.5 GPa was calculated. Although experimental data are not presently available at this pressure, the recent DFT calculations of Kress and coworkers (*31*) predict considerably different behavior in this pressure regime. The model used in the present work predicts softening behavior (v = 8.68 cm^3/mole N_2), as does the work of Fried and Howard (*11*), while the DFT calculations appear to be approaching a maximum compression in this region (v = 9.34 cm^3/mole N_2 at P = 91.5 GPa [*31*]). According to our calculations, such a system would contain a nearly equimolar mixture of N_2 molecules and dissociated N atoms (see figure 3).

5. Discussion

We have demonstrated the effectiveness of using the RxMC simulation method for determining the shock properties of materials. We found the RxMC calculations to be in excellent agreement with the available experimental data for the N_2 dissociation reaction. These results illustrate the utility of the method for predicting the shock Hugoniot for mixtures in which species concentrations are not known and in the absence of interaction potentials that simulate bond breakage and formation. In the next report of this series, we consider an application of the RxMC method to the nitric oxide decomposition reaction ($2NO \Leftrightarrow N_2+O_2$). Several possible extensions of the RxMC are also discussed in the subsequent report (*34*).

6. References

1. Touret, J.; van den Kerkhof, A. M. High Density Fluids in the Lower Crust and Upper Mantle. *Physica B & C* **1986**, *139*, 834.

2. Kortbeek, P. J.; Seldam, C. A. T.; Schouten, J. A. Calculation of Thermodynamic Properties of Dense Fluid Neon Using Statistical-Mechanical Perturbation-Theory 2 Results up to GPa and Equations of State. *Mol. Phys.* **1990**, *69*, 1001.

3. Duan, Z.; Moller, N.; Weare, J. H. A General Equation of State for Supercritical Fluid Mixtures and Molecular Dynamics Simulation of Mixture PVTX Properties. *Geochim. Cosmochim. Acta* **1996**, *60*, 1209.

4. Fickett, W.; Davis, W. C. *Detonation*; University of California Press: Berkeley, CA, 1979.

5. Ree, F. H. Supercritical Fluid Phase Separations: Implications for Detonation Properties of Condensed Explosives. *J. Chem. Phys.* **1986**, *84*, 5845.

6. Fried, L. E.; Howard, W. M. The Equation of State of Supercritical HF, HCI, and Reactive Supercritical Mixtures Containing the Elements H, C, F, and CT. *J. Chem. Phys.* **1999**, *110*, 12023.

7. Ree, F. H.; Viecelli, J. A.; van Thiel, M. Influence of Fluorine Chemistry on Supercritical Fluid-Fluid Phase Separations. *J. Mol. Liq*. **2000**, *85*, 229.

8. Ross, M. A High-Density Fluid-Perturbation Theory Based on an Inverse 12th-Power Hard-Sphere Reference System. *J. Chem. Phys.* **1979**, *71*, 1567.

9. Zerah, G.; Hansen, J. Self-Consistent Integral Equation for Fluid Pair Distribution Functions: Another Attempt. *J. Chem. Phys*. **1986**, *84*, 2336.

10. Vortler, H. L.; Nezbeda, I.; Lísal, M. The Exp-6 Potential Fluid at Very High Pressures: Computer Simulations and Theory. *Mol. Phys.* **1997**, *92*, 813.

11. Fried, L. E.; Howard, W. M. An Accurate Equation of State for the Exponential-6 Fluid Applied to Dense Supercritical Nitrogen. *J. Chem. Phys.* **1998**, *109*, 7338.

12. Ree, F. H. A Statistical Mechanical Theory of Chemically Reacting Multiphase Mixtures: Application to the Detonation Properties of PETN. *J. Chem. Phys*. **1984**, *81*, 1251.

13. Fried, L. E. *Cheetah 3.0 User's Manual*; Lawrence Livermore National Laboratory: Livermore, CA, Revision 3, 2001.

14. Karo, A. M.; Hardy, J. R.; Walker, F. E. Theoretical Studies of Shock-Initiated Detonations. *Acta Astronaut* **1978**, *5*, 1041.

15. Batteh, J. H.; Powell, J. D. Shock Propagation in One-Dimensional Lattice at a Non-Zero Initial Temperature. *J. Appl. Phys*. **1978**, *49*, 3933.

16. Batteh, J. H.; Powell, J. D. Solitary-Wave Propagation in the 3-Dimensional Lattice. *Phys. Rev. B* **1979**, *20*, 1398.

17. Powell, J. D.; Batteh, J. H. Effects of Solitary Waves Upon the Shock Profile in a 3-Dimensional Lattice. *J. Appl. Phys.* **1980**, *51*, 2050.

18. Holihan, B. L.; Hoover, W. G.; Moran, B.; Straub, G. K. Shock-Wave Structure via Nonequilibrium Molecular Dynamics and Navier-Stokes Continuum Mechanics. *Phys. Rev. A* **1980**, *22*, 2798.

19. Tsai, D. H.; Trevino, S. F. Simulation of the Initiation of Detonation in an Energetic Molecular Crystal. *J. Chem. Phys.* **1984**, *81*, 5636.

20. Tsai, D. H. *Chemistry and Physics of Energetic Materials*; Bulusu, S. N., Ed.; Kluwer: Dordrecht, 1990.

21. Brenner, D. W. Molecular Potentials for Simulating Shock-Induced Chemistry. In *Shock Compression of Condensed Matter*; Elsevier: Amsterdam, 1992.

22. Robertson, D. H.; Brenner, D. W.; Elert, M. L.; White, C. T. Simulations of Chemically Sustained Shock Fronts in a Model Energetic Material. In *Shock Compression of Condensed Matter;* Elsevier: Amsterdam, 1992.

23. White, C. T.; Robertson, D. H.; Elert, M. L.; Brenner, D. W. Molecular Dynamics Simulations of Shock-Induced Chemistry: Application to Chemically Sustained Shock Waves. In *Microscopic Simulations of Complex Hydrodynamic Phenomena*; Plenum: New York, 1992.

24. Erpenbeck, J. J. Molecular Dynamics of Detonation I. Equation of State and Hugoniot Curve for a Simple Reactive Fluid. *Phys. Rev. A* **1992**, *46*, 6406.

25. Brenner, D. W.; Robertson, D. H.; Elert, M. L.; White, C. T. Detonations at Nanometer Resolution Using Molecular Dynamics. *Phys. Rev. Lett.* **1993**, *70*, 2174.

26. White, C. T.; Sinnott, S. B.; Mintmire, J. W.; Brenner D. W.; Robertson, D. H. Chemistry and Phase Transitions From Hypervelocity Impacts. *Int. J. Quantum Chem. Symp.* **1994**, *28*, 129.

27. Rice, B. M.; Mattson, W.; Grosh, J.; Trevino, S. F. Molecular Dynamics Study of Detonation I. A Comparison With Hydrodynamic Predictions. *Phys. Rev. E* **1996**, *53*, 611.

28. Rice, B. M.; Mattson, W.; Grosh, J.; Trevino, S. F. Molecular Dynamics Study of Detonation II. The Reaction Mechanism. *Phys. Rev. E* **1996**, *53*, 623.

29. Maillet, J. B.; Mareschal, M.; Soulard, L.; Ravelo, R.; Lomdahl, P. S.; Germann, T. C.; Holian, B. L. Uniaxial Hugoniostat: A Method for Atomistic Simulations of Shocked Materials. *Phys. Rev. E* **2000**, *63*, 016121.

30. Swanson, D. R.; Mintmire, J. W.; Robertson, D. H.; White, C. T. Detonation Hugoniots from Molecular Dynamics Simulations. *Chem. Phys. Reps.* **2000**, *18*, 1871.

31. Kress, J. D.; Mazevet, S.; Collins, L. A.; Wood, W. W. Density-Functional Calculation of the Hugoniot of Shocked Nitrogen. *Phys. Rev. B.* **2000**, *63*, 024203.

32. Johnson, J. K.; Panagiotopoulos, A. Z.; Gubbins, K. E. Reactive Canonical Monte Carlo - A New Simulation Technique for Reacting or Associating Fluids. *Mol. Phys.* **1994**, *81*, 717.

33. Smith, W. R.; Tříska, B. J. The Reaction Ensemble Method for the Computer Simulation of Chemical and Phase Equilibria. I. Theory and Basic Examples. *Chem. Phys.* **1994**, *100*, 3019.

34. Brennan, J. K.; Rice, B. M. Molecular Dynamics Simulations of SiO_2. U.S. Army Research Laboratory: Aberdeen Proving Ground, MD, submitted for publication, 2005.

35. Reed, T. M.; Gubbins, K. E. *Applied Statistical Mechanics*; McGraw-Hill: New York, NY, 1973.

36. McQuarrie, D. A. *Statistical Mechanics*; Harper: New York, NY, 1976.

37. Chase, M. W.; Davies, C. A.; Downey, J. R.; Frurip, D. J.; McDonald, R. A.; Syverud, A. N. *JANAF Thermochemical Tables*, Third Edition, *J. Phys. Chem.* Ref. Data **1985**, *14*.

38. Johnson, J. K. Reactive Canonical Monte Carlo. *Adv. Chem. Phys.* **1999**, *105*, 461.

39. Lísal, M.; Smith, W. R. Institute of Chemical Process Fundamentals, Academy of Sciences of the Czech Republic. Private communication, 2002.

40. Lísal, M.; Nezbeda, I.; Smith, W. R. The Reaction Ensemble Method for the Computer Simulation of Chemical and Phase Equilibria. II. The Br_2 + Cl_2 + BrCL System. *J. Chem. Phys.* **1999**, *110*, 8597.

41. Lísal, M.; Smith, W. R.; Nezbeda, I. Accurate Computer Simulation of Phase Equilibrium for Complex Fluid Mixtures. Application to Binaries Involving Isobutene, Methanol, Methyl Tert-Butyl Ether, and N-Butane. *J. Phys. Chem. B* **1999**, *103*, 10496.

42. Lísal, M.; Smith, W. R.; Nezbeda, I. Computer Simulation of the Thermodynamic Properties of High-Temperature Chemically-Reacting Plasmas. *J. Chem. Phys.* **2000**, *113*, 4885.

43. Turner, C. H.; Johnson, J. K.; Gubbins, K. E. Effects of Confinement on Chemical Reaction Equilibria: The Reaction $2NO \Leftrightarrow (NO)_2$ and $N_2 + 3H_2 \Leftrightarrow 2NH_3$ in Carbon Micropores. *J. Chem. Phys.* **2001**, *114*, 1851.

44. Borówko, M.; Zagórski, R. Chemical Equilibria in Slit-Like Pores. *J. Chem. Phys.* **2001**, *114*, 5397.

45. Turner, C. H.; Brennan, J. K.; Johnson, J. K.; Gubbins, K. E. Effects of Confinement by Porous Materials on Chemical Reaction Kenetics. *J. Chem. Phys.* **2002**, *116*, 2138.

46. Turner, C. H.; Brennan, J. K.; Pikunic, J. P.; Gubbins, K. E. Simulation of Chemical Reaction Equilibria and Kinetics in Heterogeneous Carbon Micropores. *App. Surf. Sci.*, in press, 2002.

47. Metropolis, N.; Rosenbluth, A. W.; Rosenbluth, M. N.; Teller, A. E.; Teller, E. Equation of State Calculations by Fast Computing Machines. *J. Chem. Phys.* **1953**, *21*, 1087.

48. Lofthus, A.; Krupenie, P. H. *J. Phys. Chem.* Ref. Data, **1977**, *6*, 113.

49. Moore, C. E.; Gallagher, J. W. *Tables of Spectra of Hydrogen, Carbon, Oxygen Atoms and Ions, CRC Series in Evaluated Data in Atomic Physics*; Chemical Rubber: Boca Raton, FL, 1993.

50. Curtiss, L. A.; Redfern, P. C.; Furip, D. J. *Reviews in Computational Chemistry*; Lipkowitz K. B., Boyd, D. B., Eds.; Wiley-VCH, John Wiley and Sons, Inc.: New York, NY, 2000; Vol. 15, pp 147.

51. Ochterski, J. W. Thermochemistry in Gaussian. http://www.gaussian.com (accessed 2000), Gaussian, Inc.

52. Frenkel, D.; Smit, B. *Understanding Molecular Simulation*; Academic Press: San Diego, CA, 1996.

53. Allen, M. P.; Tildesley, D. J. *Computer Simulation of Liquids*; Oxford University Press: Oxford, UK, 1987.

54. Zubarev, V. N.; Telegin, G. S. Calculation of Parameters of Detonation Waves From Condensed Explosives. *Sov. Phys. Dokl*. **1962**, *7*, 34.

55. Nellis, W. J.; Radousky, H. B.; Hamilton, D. C.; Mitchell, A. C.; Holmes, N. C.; Christianson, K. B.; van Thiel, M. Equation-of-State, Shock-Temperature, and Electrical-Conductivity Data of Dense Fluid Nitrogen in the Region of the Dissociative Phase Transition. *J. Chem. Phys.* **1991**, *94*, 2244.

56. Radousky, H. B.; Nellis, W. J.; Ross, M.; Hamilton, D. C.; Mitchell, A. C. Molecular Dissociation and Shock-Induced Cooling in Fluid Nitrogen at High Densities and Temperatures. *Phys. Rev. Lett.* **1986**, *57*, 2419.

57. Ross, M. The Dissociation of Dense Liquid Nitrogen. *J. Chem. Phys.* **1987**, *86*, 7110.

58. McMahan, A. K.; LeSar, R. Pressure Dissociation of Solid Nitrogen Under 1 Mbar. *Phys. Rev. Lett.* **1985**, *54*, 1929.

59. Martin, R. M.; Needs, R. J. Revision B, **1986**, *34*, 5082.

60. van Thiel, M.; Ree, F. H. Accurate High-Pressure and High-Temperature Effective Pair Potentials for the Systems N_2–N and O_2–O. *J. Chem. Phys.* **1986**, *104*, 5019.

61. Hamilton, D. C.; Ree, F. H. Chemical Equilibrium Calculations on the Molecular-to-Nonmolecular Transition of Shock Compressed Liquid Nitrogen. *J. Chem. Phys.* **1989**, *90*, 4972.

62. Ross, M. Shock Compression of Simple Liquids: Implications for Deuterium. *High Press. Res.* **2000**, *16*, 371.

NO. OF COPIES	ORGANIZATION
1 (PDF ONLY)	DEFENSE TECHNICAL INFORMATION CTR DTIC OCA 8725 JOHN J KINGMAN RD STE 0944 FORT BELVOIR VA 22060-6218
1	US ARMY RSRCH DEV & ENGRG CMD SYSTEMS OF SYSTEMS INTEGRATION AMSRD SS T 6000 6TH ST STE 100 FORT BELVOIR VA 22060-5608
1	DIRECTOR US ARMY RESEARCH LAB IMNE ALC IMS 2800 POWDER MILL RD ADELPHI MD 20783-1197
3	DIRECTOR US ARMY RESEARCH LAB AMSRD ARL CI OK TL 2800 POWDER MILL RD ADELPHI MD 20783-1197

ABERDEEN PROVING GROUND

1	DIR USARL AMSRD ARL CI OK TP (BLDG 4600)

NO. OF COPIES	ORGANIZATION
1	DIRECTOR US ARMY RESEARCH LAB AMSRD ARL D J MILLER 2800 POWDER MILL RD ADELPHI MD 20783-1197
2	DIRECTOR US ARMY RESEARCH LAB AMSRD ARL RO P R SHAW TECH LIB PO BOX 12211 RESEARCH TRIANGLE PARK NC 27709-2211
1	CDR US ARMY ARDEC TECH LIB PICATINNY ARSENAL NJ 07806-5000
1	CDR NAVAL RSRCH LAB TECH LIBRARY WASHINGTON DC 20375-5000
1	OFFICE OF NAVAL RSRCH J GOLDWASSER 875 N RANDOLPH ST RM 653 ARLINGTON VA 22203-1768
1	CDR NAVAL SURFACE WARFARE CTR TECH LIB INDIAN HEAD MD 20640-5000
1	CDR NAVAL SURFACE WARFARE CTR TECH LIB DAHLGREN VA 22448-5000
1	AIR FORCE RSRCH LAB MNME EN MAT BR B WILSON 2306 PERIMETER RD EGLIN AFB FL 32542-5910
1	AIR FORCE OFC OF SCI RSRCH M BERMAN 875 N RANDOLPH ST STE 235 RM 3112 ARLINGTON VA 22203-1768

NO. OF COPIES	ORGANIZATION
1	DIR SANDIA NATL LABS M BAER DEPT 1512 PO BOX 5800 ALBUQUERQUE NM 87185
1	DIR LAWRENCE LIVERMORE NL L FRIED PO BOX 808 LIVERMORE CA 94550-0622
1	UNIV OF ALABAMA DEPT OF CHEMICAL ENGRG C TURNER A132 BEVILL TUSCALOOSA AL 35487-0286
	ABERDEEN PROVING GROUND
61	DIR USARL AMSRD ARL WM T ROSENBERGER AMSRD ARL WM M S MCKNIGHT AMSRD ARL WM T B BURNS AMSRD ARL WM TB P BAKER AMSRD ARL WM BD R ANDERSON W ANDERSON R BEYER A BRANT G BROWN S BUNTE C CANDLAND W CIEPIELA G COOPER L CHANG T COFFEE J COLBURN P CONROY B DAVIS J DESPIRITO N ELDREDGE B FORCH J GARNER D HEPNER B HOMAN A HORST

NO. OF COPIES	ORGANIZATION
	S HOWARD
	P KASTE
	G KATULKA
	T KOGLER
	A KOTLAR
	C LEVERITT
	R LIEB
	D LYON
	K MCNESBY
	M MCQUAID
	M MILLER
	A MIZIOLEK
	J MORRIS
	J NEWBERRY
	J NEWILL
	M NUSCA (6 CPS)
	W OBERLE
	R PESCE-RODRIGUEZ
	P PLOSTINS
	S PIRIANO
	G REEVES
	B RICE
	J SAHU
	R SAUSA
	S SILTON
	E SCHMIDT
	J SCHMIDT
	P WEINACHT
	D WILKERSON
	A WILLIAMS
	M ZOLTOSKI

NO. OF COPIES	ORGANIZATION
1	ACADEMY OF SCIENCES OF THE CZECH REPUBLIC E HALA LABORATORY OF THERMODYNAMICS M LISAL 165 02 PRAGUE 6-SUCHDOL CZECH REPUBLIC

INTENTIONALLY LEFT BLANK.